

Influence of distinct kinds of temporal disorder in discontinuous phase transitions

Jesus M. Encinas and C. E. Fiore^{1*}

¹ *Instituto de Física, Universidade de São Paulo,
Caixa Postal 66318
05315-970 São Paulo, São Paulo, Brazil*
(Dated: October 1, 2020)

Based on the MFT arguments, a general description for discontinuous phase transitions in the presence temporal disorder is considered. Our analysis extends the recent findings [Phys. Rev. E **98**, 032129 (2018)] by considering other kinds of phase transitions beyond the absorbing ones. The theory is exemplified in the simplest (nonequilibrium) order-disorder (discontinuous) phase transition with "up-down" Z_2 symmetry: the inertial majority vote (IMV) model for two kinds of temporal disorder. As for the APT case, the temporal disorder does not suppress the occurrence of discontinuous phase transitions, but remarkable differences emerge when compared with the pure case. A comparison between the distinct kinds of temporal disorder is also performed beyond the MFT for random-regular (RR) complex topologies.

I. INTRODUCTION

Disorder due inhomogeneities is present in many real systems and commonly plays a significant role in their behaviors [1–3]. In the last years, many attention has been devoted for critical phase transitions in the presence of spatial [4–8] and temporal disorders [9–15], in which one has established the existence of new (and universal) critical behaviors. Remarkably, both kinds of disorder are also characterized by the existence a subregion of phase space in which one observes exotic behaviors. The former is named spatial Griffiths phase and corresponds to a subregion in the absorbing phase in which the order parameter vanishes slower than (power-law or stretched exponential) the exponential decay in the absence of disorder. Conversely, temporal disorder is featured by a region in the active phase in which the mean lifetime increases as a power-law (instead of exponential).

Spontaneous breaking symmetry manifests in a countless sort of systems beyond the classical ferromagnetic-paramagnetic phase transition [1, 2]. It includes remarkable examples, such as school fishes moving under an ordered way for protecting themselves against predators, spontaneous formations of a common language and culture, the emergence of consensus [16–18] in social systems and other remarkable examples. Such phase transitions are typically critical and belong to well established universality classes [1–3, 19]. A remarkable example commonly considered for modeling/describing some of above phenomena is the majority vote (MV) model [19–21], in which a local spin tends to align itself with its local neighborhood majority spins. Originally, it presents a continuous phase transition belonging to distinct universality classes, according to the lattice topology [19–21]. More recently [22–24], it has been found that the inclusion of inertia in the MV (IMV), e.g. a term proportional to the local spin, can shift the phase transition to a discontinuous phase transition in complex networks [22, 23]

or even in regular lattices [24, 25]. The importance of such results is highlighted by the fact that behavioral inertia is an essential characteristic of human being and animal groups and it is also a significant ingredient triggering abrupt transitions that arise in social systems [16]. However, the effects under the inclusion of more realistic ingredients, such its time dependent variation, have not been satisfactorily understood yet.

Recently, a theory for discontinuous absorbing phase transitions (APTs) in the presence of temporal disorder has been proposed in Ref. [26]. In contrast to the spatial disorder case [27], discontinuous APTs are not suppressed due to the temporal disorder, although remarkable features emerge when compared with their pure (disorderless) systems. Giving that systems with Z_2 "up-down" symmetry display remarkably different features from APTs (which can be viewed in terms of the simple logistic order-parameter x equations: $dx/dt = ax - bx^2 + cx^3 \dots$ (APT) and $dx/dt = ax - bx^3 + cx^5 \dots$ (Z_2) [28]), a question that naturally arises is if similar findings are verified/can be extended beyond the APT. Additionally, a second important point concerns at a comparison between distinct kinds of temporal disorder. In the specific case of IMV, giving that the inertia plays a fundamental role for shifting the phase transition, we intend to tackle the effect of temporal disorder in the inertia and their differences respect to the (usual) control parameter case.

Aimed at answering aforementioned points, here we examine, separately, the role of temporal disorder in two fundamental ingredients: the control parameter and inertia. Based on mean-field analysis, we derive general predictions for both kinds of temporal disorder, which are also verified beyond in the MFT for complex structures.

This paper is organized as follows: In Sec. II we present the analysis of pure model and temporal disorder based on the MFT, in Sec. III we present the main findings beyond the MFT. Conclusions are drawn in Sec. IV.

* fiore@if.usp.br

II. MODEL AND MEAN FIELD ANALYSIS

The original (inertialess) majority vote model (MV) is defined as follows. At each time step, a site i with spin σ_i is randomly selected and with probability $1 - f$ it is aligned with the majority of its k_i nearest-neighbors and with the complementary probability f the majority rule is not followed. The inertial majority vote model (IMV) differs from the MV for the inclusion of an inertial term θ , taking into account the contribution of the local spin. In such a case, the probability of following the majority rule will also depend on the local spin σ_i , whose transition rate $\omega_i(\sigma)$ from $\sigma_i \rightarrow -\sigma_i$ is given by [22]

$$\omega(\sigma_i) = \frac{1}{2} [1 - (1 - 2f)\sigma_i S(\Theta_i)], \quad (1)$$

where Θ_i accounts for the local neighborhood plus the inertial contribution given by

$$\Theta_i = (1 - \theta) \sum_{j=1}^{k_i} \frac{\sigma_j}{k_i} + \theta \sigma_i,$$

with $S(x) = \text{sign}(x)$ if $x \neq 0$ and $S(0) = 0$. Note that one recovers the original MV when $\theta = 0$ and an order-disorder phase transition yields only when the inertia is constrained between $\theta \in [0, 0.5]$. For $\theta = 0.5$ the system gets frozen in the order/disorder phase according to whether $f = 0/f \neq 0$. By increasing θ and the connectivity, phase transition is shifted from a continuous (second-order) to a discontinuous (first-order). At the mean-field level the phase coexistence is marked by the appearance of an hysteretic region in which two symmetric ordered and a disordered phases coexist. Such features are also manifested in complex networks but an entirely different behavior is presented for regular lattices [24], in which quantities scale with the system volume.

From the transition rate, the time evolution of the average magnetization $m_k = \langle \sigma_i \rangle_k$ of a local site i with degree k is given by

$$\frac{d}{dt} m_k = -m_k + (1 - 2f) \langle S(\Theta_i) \rangle. \quad (2)$$

The first analysis will be performed by means of a MFT treatment, in which the joint probabilities appearing in the average $\langle S(\Theta_i) \rangle$ are a rewritten in terms of one-site probabilities. From this assumption, one arrives the following expression $\langle S(\Theta_i) \rangle = (1 + m_k) \langle S(\Theta_+) \rangle / 2 + (1 - m_k) \langle S(\Theta_-) \rangle / 2$, where $\langle S(\Theta_{\pm}) \rangle$ are given by

$$\langle S(\Theta_{\pm}) \rangle \approx \sum_{n=[n_k^{\pm}]}^k C_n^k p_+^n p_-^{k-n} - \sum_{n=[n_k^{\mp}]}^k C_n^k p_-^n p_+^{k-n}, \quad (3)$$

with p_{\pm} being the probability that a nearest neighbor is ± 1 (in which one associates the local magnetization $p_{\pm} = (1 \pm m^*)/2$) and n_k^- and n_k^+ correspond to the lower limit of the ceiling function given by $n_k^- = k/[2(1 - \theta)]$ and $n_k^+ = k(1 - 2\theta)/[2(1 - \theta)]$, respectively.

In order to relate m^* and m_k , we shall focus our analysis on uncorrelated networks, in which the probability of a randomly chosen site has degree k reads $kP(k)/\langle k \rangle$, with $P(k)$ and $\langle k \rangle$ being the probability distribution of nodes and its mean degree $\langle k \rangle$, respectively. The relation between m^* and m_k then reads $m^* = \sum_k m_k k P(k) / \langle k \rangle$. By combining above expression with Eq. (2), we obtain the following self-consistent equation of m^* in the steady-state regime:

$$m^* = (1 - 2f) \sum_k \frac{kP(k)}{\langle k \rangle} \left[\left(\frac{1 + m_k}{2} \right) \langle S(\Theta_+) \rangle + \left(\frac{1 - m_k}{2} \right) \langle S(\Theta_-) \rangle \right] \quad (4)$$

Above expression can be analyzed for distinct complex structures. For a random-regular (RR) topology, $P(k)$ is given by $P(k) = \delta(k - k_0)$ and hence all sites have the same number of neighbors k_0 , from which one arrives at the following expression for the steady $m^* = m(k_0) \equiv m$ in terms of f and θ :

$$m = (1 - 2f) \left[\left(\frac{1 + m}{2} \right) \langle S(\Theta_+) \rangle + \left(\frac{1 - m}{2} \right) \langle S(\Theta_-) \rangle \right]. \quad (5)$$

Above expressions present two and three stable solutions in the case of continuous and discontinuous phase transitions, marked at $f = f_c$ (critical point) and $f = f_f$ (order-parameter jump), respectively. In both cases, there is a trivial solution, $f > f_c$ ($f > f_f$) corresponding to the disordered (DIS) phase: $m(t \rightarrow \infty) = m_d(f) = 0$, irrespectively on the initial condition. Conversely, for $f < f_b$, the system evolves to $m(t \rightarrow \infty) \rightarrow m_s(f)$, also independently on the initial condition. The third solution $m_u(f)$ is called unstable solution and appears for values of f constrained in the interval $f_b < f < f_f$. More specifically, $m(t \rightarrow \infty) \rightarrow m_s(f)$ and $m(t \rightarrow \infty) \rightarrow m_d(f)$, if $m(0) > m_u(f)$ and $m(0) < m_u(f)$, respectively. This feature of the ordered phase will be referred as the metastable (ME) phase, contrasting with the behavior for $f < f_b$. Although the discontinuous phase transition yields at $f = f_f$, the region $f = f_b$ marks the crossover between an ordered phase characterized by bistable and monostable behaviors for $f_b < f < f_f$ and $f < f_b$, respectively. Since $m(t)$ deviates from $m_u(f)$ whenever $m(0) \neq m_u(f)$, such a solution is unstable.

Although analytic expressions and the stability of solutions based on Eqs. (4) and (5) are quite cumbersome, a simpler analysis can be performed in the limit of large connectivities, since each term of the binomial distribution approaches a Gaussian with mean $k p_{\pm}$ and variance $\sigma^2 = k p_+ p_-$ [20, 23, 29–31]. From Eq. (5), the first term from the right side is approximately rewritten as

$$\begin{aligned} \sum_{n=[n_k^{\pm}]}^{k_0} C_n^{k_0} p_{\pm}^n p_{\mp}^{k_0-n} &\rightarrow \frac{1}{\sigma \sqrt{2\pi}} \int_{n_k^+}^{k_0} e^{-\frac{(\ell - k_0 p_{\pm})^2}{2\sigma^2}} d\ell = \\ &= \frac{1}{2} \sqrt{\pi} \left\{ \text{erf} \left[\frac{k_0(1 - p_{\pm})}{\sqrt{2}\sigma} \right] - \text{erf} \left[\frac{k_0(n_k^+ - p_{\pm})}{\sqrt{2}\sigma} \right] \right\}, \quad (6) \end{aligned}$$

with $\text{erf}(x)$ denoting the error function $\text{erf}(x) = 2 \int_0^x e^{-t^2} dt / \sqrt{\pi}$, and the second one can be rewritten under a similar way. Taking into account that $\text{erf}[k_0(1 -$

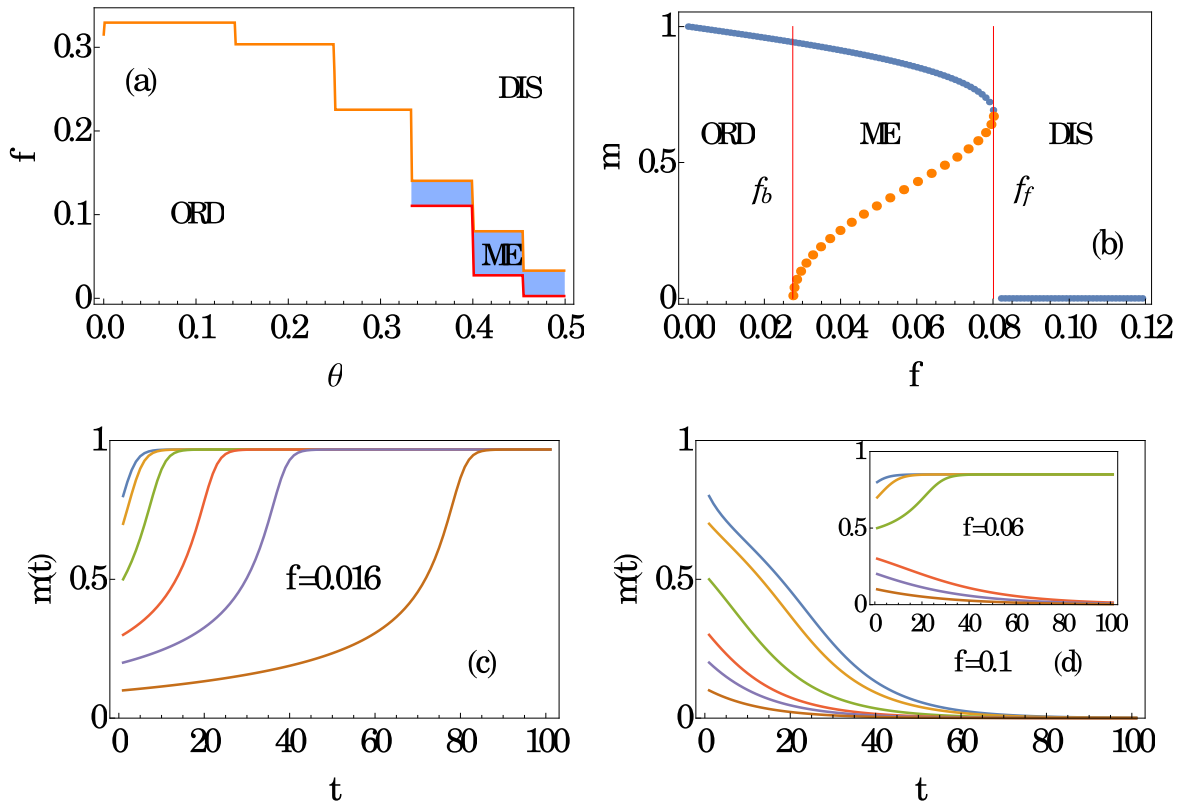


FIG. 1. Panel (a) depicts the MFT phase diagram for a RR topology with $k_0 = 12$. ORD/ME and DIS denote the ordered monostable/bistable and disordered phases, respectively. In (b), the behavior of average magnetization m versus f for $\theta = 0.45$. Continuous and dashed lines denote to the stable and unstable solutions of Eq. (5), respectively. Their main features are exemplified in panels (c) – (d) by taking the time evolution of m as a function of time for $f = 0.016$ (c), $f = 0.10$ (d) and 0.06 (inset) for distinct initial conditions $m(0)$.

$p_{\pm})/\sqrt{2}\sigma]$ approaches to 1 for large k_0 , we arrive at the following expression for the steady state regime:

$$f = \frac{1}{2} \left[1 - \frac{2m}{(1+m)\text{erf}(\alpha) - (1-m)\text{erf}(\beta)} \right], \quad (7)$$

with parameters α and β given by

$$\alpha = \sqrt{\frac{k_0}{2}} \left[\frac{\theta}{1-\theta} + m \right] \quad \text{and} \quad \beta = \sqrt{\frac{k_0}{2}} \left[\frac{\theta}{1-\theta} - m \right]. \quad (8)$$

The transition point f_f can be obtained from the maximum of Eq. (7). At the vicinity of f_b (or f_c for a critical phase transition), m is expected to be small and hence one has the following logistic equation $dm/dt \approx A(f, \theta, k_0)m$, with $A(f, \theta, k_0)$ given by

$$A(f, \theta, k_0) = -1 + (1-2f) \left[\sqrt{\frac{2k_0}{\pi}} e^{-\frac{k_0 \theta^2}{2(1-\theta)^2}} + \text{erf} \left(\sqrt{\frac{k_0}{2}} \frac{\theta}{1-\theta} \right) \right]. \quad (9)$$

From the above expression, f_b is then given by $A(f_b, \theta, k_0) = 0$. Note that one reduces to the expression $2f_c = 1 - \sqrt{\pi/(2k)}$, when $\theta = 0$ [20, 30]. Hence, $m(t)$ is exponentially increasing towards its steady state value $m_s(f)$ if $A(f, k_0, \theta) > 0$ ($f < f_b$) and vanishes exponentially for $A(f, k_0, \theta) < 0$, ($f_b < f < f_f$), respectively, if $m(0) \ll 1$ [see e.g. Figs .1(c) and (d)(inset)]. Since $f_f > f_b$, $m(t)$ also vanishes exponentially towards $m_d(f)$.

In order to illustrate all previous findings, Fig. 1 depicts, for the clean system, the phase diagram and all above main features of discontinuous phase transitions for $k_0 = 12$ and $\theta = 0.45$ as f is changed. In particular, the regions $f \leq f_b = 0.0274573\dots$ and $f_b < f < f_f = 0.080121$ mark the ORD and ME phases, respectively, whereas for $f > f_f$ the disordered phase (DIS) prevails. Similar results are obtained for other connectivities k_0 and θ .

As a final remark, it is worth mentioning that although the dependence between m and θ is more cumbersome than with f , all previous findings are hold valid when the inertia is taken as the control parameter (for fixed f).

A. Temporal disorder in the control parameter

Once presented the main features about the pure system, we now are in position for tackling the effects of the temporal disorder. We start with time variations of the control parameter f . Although similar findings are expected for distinct temporal disorder distributions, we shall consider a simplest case in which for a given time interval constrained between t and $t + \Delta t$, control parameter f is randomly extracted from a bimodal distribution $P_{dis}(f)$:

$$P_{dis}(f) = p\delta(f - f_-) + (1 - p)\delta(f - f_+), \quad (10)$$

where $f_- < f_+$ and $p(1 - p)$ is the probability in which f assumes the values $f_-(f_+)$. During this time interval, the system behaves as the pure system, since its control parameter is kept fixed. For simplicity and also for comparing with previous findings [26], we set $p = 1/2$.

Analysis starts from a given initial condition $m(0)$ and its time evolution is analyzed until a sufficient large time t_{max} in which one has generated a given sequence of control parameter values $\{f_1, f_2, \dots, f_M\}$, where $t_{max} = M \times \Delta t$. This process is then repeated for sufficiently N_D distinct disorder sequences (we have considered here $N_D = 10^2 - 10^3$).

Next, we analyze the cases in which f_- and f_+ belong to different phases. Starting with $f_- \in \text{ORD}$ and $f_+ \in \text{ME}$ (with $f_- < f_b$ and $f_b \leq f_+ \leq f_f$), the phase predominance can be understood under a heuristic analysis, based on the time evolution for $m(t) \ll 1$. By recalling that $m(t)$ will increase/decrease exponentially as $m \sim e^{\alpha(f_b - f_-)t}$ and $m \sim e^{-\alpha(f_+ - f_b)t}$ [with α and f_b given approximately by Eq. (9) for large k_0], respectively, the dynamics will be then characterized for sequences of exponentially increasing and vanishing behaviors, in which the ordered phase prevails if $f_+ + f_- < 2f_b$, whereas the metastable phase dominates when $f_+ + f_- > 2f_b$. The line fulfilling $f_+ + f_- = 2f_b$ denotes the crossover between ordered and metastable phases lines.

We next consider the case in which f_- and f_+ belong to the ME and DIS phases, respectively. Although logistic equations are different from absorbing phase transitions [26], the hysteretic branch makes the disordered phase prevailing over metastable one. Since the magnetization

Although our findings are not dependent on the value of k_0 and θ , the effect of temporal disorder will be exemplified for $k_0 = 12$ and $\theta = 0.45$, in order to compare both clean and disordered systems. All possible variations of both f_- and f_+ along ORD, ME and DIS will be considered. We face two scenarios, in which both f_- and f_+ belong to the same and different phases, respectively.

Let us start with the case when both f_- and f_+ varies over the ordered phase ($0 \leq f_{\pm} < f_b$). Irrespective on the initial condition $m(0)$ the system will evolve towards an ordered state in which the steady magnetization fluctuates between $m_s(f_-)$ and $m_s(f_+)$. A similar conclusion is valid for both f_- and f_+ belong to the disordered phase ($f_f < f_{\pm} \leq 1/2$), in which the disordered phase prevails independently on $m(0)$. For both f_- and f_+ belonging to the metastable phase ($f_b \leq f_{\pm} \leq f_f$ and $m_u(f_-) < m_u(f_+)$), then $m(t \rightarrow \infty) \rightarrow 0$ and $m(t \rightarrow \infty) \neq 0$ if $m(0) < m_u(f_-)$ and $m(0) > m_u(f_+)$, respectively, irrespective the sequence of f_- and f_+ , respectively. The case in which $m_u(f_-) \leq m(0) \leq m_u(f_+)$ will depend on the particular sequence of f_- and f_+ . This can be verified under two extreme cases. Take for instance a particular (long) sequence of $f = f_+$, in which $m(t)$ becomes lower than $m_u(f_-)$. In such a case, the system always reaches the disordered phase. Conversely a long sequence of $f = f_-$ will lead to $m(t) > m_u(f_+)$ and then the system will converge to the ordered phase. Thus, as for absorbing phase transitions [26], ORD, ME and DIS phases are preserved under the temporal disorder.

vanishes irrespectively the initial condition for $f > f_f$, it suffices a single long sequence of consecutive (e.g. a rare fluctuation) f_+ 's in which $m(t) < m_u(f_-)$ for the system reaching the disordered phase. For a sufficient long time, a rare fluctuation occurs with probability one and thus the temporal disorder will suppress the ME phase whenever $f_+ < f_f$. A discontinuous phase transition between DIS and ME phases yields at $f_+ = f_f^-$. Such features are appraised in Figs. 2 (c) for distinct realizations. Despite the prevalence of the disorder phase, the average behavior $m(t)$ (measured over many runs) is very different from individual runs and it is characterized by a long period of a system exhibits ordering until vanishing, as depicted in Figs. 2 (d). Note that the time required for the appearance of a rare fluctuation increases by lowering Δt . Thus, such (rare) temporal fluctuations dramatically change the behavior of metastable phase, whose vanishing behavior towards the disordered phase is expected to be similar that for APTs [26].

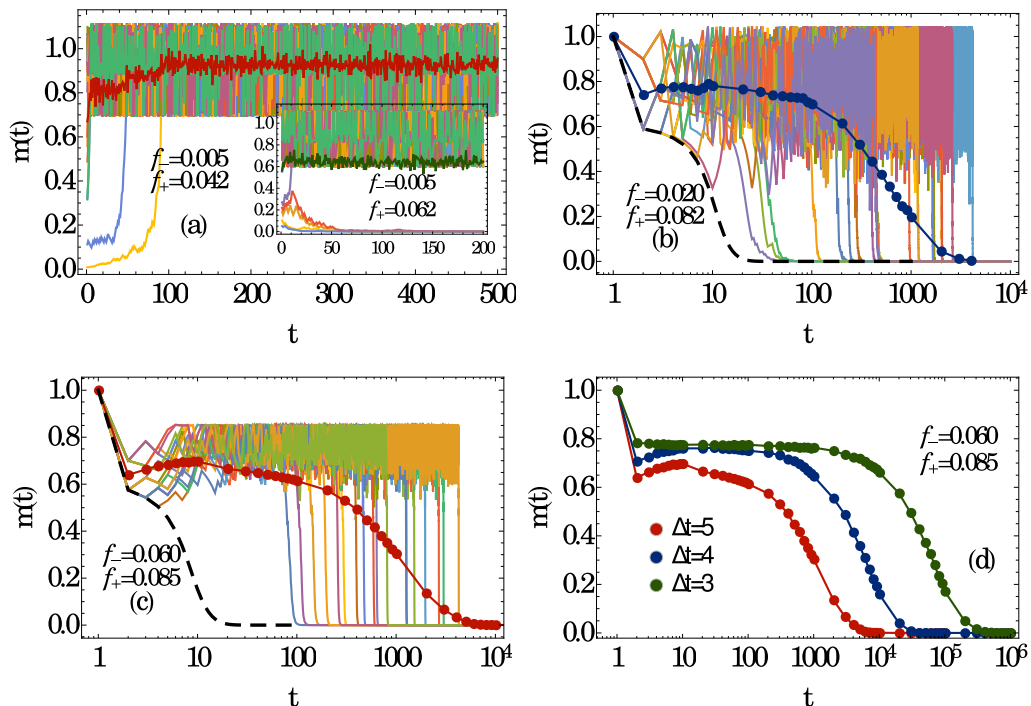


FIG. 2. MFT temporal disorder analysis: For a RR network with $k_0 = 12$, $\theta = 0.454$ and $\Delta t = 5$ the time evolution of m for distinct sets of f_+ and f_- and distinct independent realizations. Panel (a) – (c) exemplifies the following cases: $(f, f_+) \in (\text{ORD}, \text{ME})$ with $\bar{f} < f_b$ and $\bar{f} > f_b$ (inset), $(f_-, f_+) \in (\text{ORD}, \text{DIS})$ and $(f_-, f_+) \in (\text{ME}, \text{DIS})$, respectively. Dashed and symbol curves correspond to the pure versions (for $f = f_+$) and m averaged over $N_D = 10^3$ realizations, respectively. Panel (d) shows m averaged for $\Delta t = 3, 4$ and 5 .

When f_- and f_+ belong to the ORD and DIS phases, the resulting phase can also be understood from the competition between deterministic increasing and vanishing behaviors at $m(t) \ll 1$, in similarity with competition between the ORD and ME cases. Thereby, the ordered and disordered phase will prevail if $\bar{f} < f_b$ and $\bar{f} > f_b$, respectively, where $2f_b = f_+ + f_-$ marks the separatrix between above regimes. As previously, the average $m(t)$ is significantly different from individual runs and its vanishment also yields for longer times as Δt decreases. These features are exemplified in Fig. 2(b) for $f_- = 0.020$ and $f_+ = 0.082$, $N_D = 20$ individual runs and $\Delta t = 5$. As it can be seen, all realizations and its average value (symbol curves) remarkably differs from the pure version (dashed lines). The prevalence of ORD phase is possible only for smaller values of inertia ($1/3 < \theta < 2/5$ and $3/13 < \theta < 1/3$ for $k_0 = 12$ and $k_0 = 20$, respectively). In particular for $k_0 = 12$ and $\theta = 0.45$, the phase DIS always dominates over the ORD phase, since the lowest $f_- = 0$ and $f_+ = f_f$ are always greater than $2f_b$.

From the previous analysis, we build the diagram for the temporal disorder IMV for $k_0 = 12$ and $\theta = 0.45$, as depicted in Fig.3. Dotted and dashed lines denote the crossover and phase coexistence lines between ORD/ME and DIS/ME phases, respectively. Thereby, our findings show that APT and up-down systems shares distinct symmetry features, the effect of temporal disorder

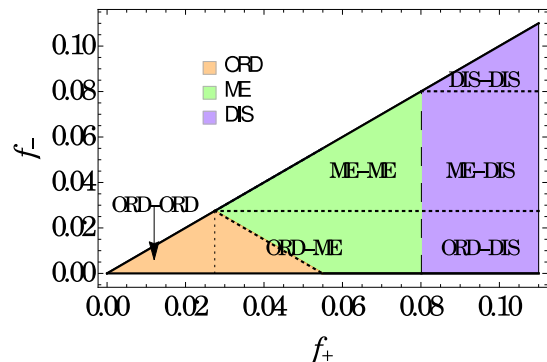


FIG. 3. MFT phase diagram for RR network with values $k_0 = 12$ and $\theta = 0.45$ under temporal disorder over the control parameter f . The resulting phase is represented by distinct colors. Dotted and dashed lines represent crossovers and discontinuous transition lines, respectively.

are similar and are directly related to the bistability of the active/ordered phase.

B. Temporal disorder in the inertia

Now we consider the effects of temporal disorder in the inertia, in which its values are chosen from two possible

values θ_- and θ_+ (with $\theta_+ > \theta_-$):

$$P_{dis}(\theta) = p\delta(\theta - \theta_-) + (1 - p)\delta(\theta - \theta_+). \quad (11)$$

Although the dependence between the $m(t)$ and θ is more cumbersome than the control parameter f , we also consider Eq. (2) in the limit of $m(0) \ll 1$, in which one has a linear equation $dm/dt = A'(f, \theta, k_0)m$. As mentioned previously, the coefficient $A'(f, \theta, k_0)$ approaches to Eq. (9) for large k_0 . In particular, $A'(f, \theta, k_0) > (< 0)$ according to whether θ belongs to the ORD (ME/DIS) phases [see e.g. Tables I, II and Eq. (9)]. For $\theta = \theta_-$ and θ_+ , $m(t)$ then behaves as $m(t) \sim e^{A'(f, \theta_-, k_0)t}$ and $m(t) \sim e^{A'(f, \theta_+, k_0)t}$, respectively, and thereby the of inertial disorder can be analyzed in similarity with the temporal disorder in f . The resulting phase then can be predicted from the competition between distinct behaviors.

Table I and Fig. 4(d) exemplifies coefficients $A'(f, \theta, k_0)$ and the phase diagram for $f = 0.12$ and distinct θ 's, respectively. For the pure version, the crossover between ORD and ME phases yields at $\theta_b = 1/3$ and ME-DIS discontinuous phase transition yields at $\theta_f = 2/5$ (see e.g. 1(a)).

TABLE I. Coefficients $A'(f, \theta, k_0)$ for $f = 0.12$ and $k_0 = 12$ and the resulting phase.

θ	$A'(f, \theta, k_0)$	phase
$0 < \theta < 1/7$	0.614...	ORD
$1/7 < \theta < 1/4$	0.467...	ORD
$1/4 < \theta < 1/3$	0.192...	ORD
$1/3 < \theta < 2/5$	-0.0122...	ME
$2/5 < \theta < 5/11$	-0.0979...	DIS
$5/11 < \theta < 1/2$	-0.118...	DIS

Starting with θ_- and θ_+ belonging to the same phase (ORD/ME/DIS) the resulting phase will be preserved for the temporal disorder, as expected. When θ_- and θ_+ belong to distinct phases, the result phase will depend on the signal of coefficients.

The case in which θ_- and θ_+ belong to ORD and ME/DIS phases, the resulting phase will be ordered if $A'(f, \theta_-, k_0) > A'(f, \theta_+, k_0)$ and ME/DIS if $A'(f, \theta_-, k_0) < A'(f, \theta_+, k_0)$, respectively.

III. BEYOND THE MEAN-FIELD THEORY: MONTE CARLO SIMULATIONS FOR DISTINCT KINDS OF TEMPORAL DISORDER

In this section, we tackle the influence of temporal disorder beyond the MFT, by analyzing its effect in complex networks structures. We also consider random-regular structures which have been built for fixed connectivity

The competition between θ_- and θ_+ belonging to the ME and DIS phases will also result in the disordered phase. Since both $A'(f, \theta_-, k_0)$ and $A'(f, \theta_+, k_0)$ are negative, the system solely requires a long sequence of $\theta = \theta_+$ for driving it to $m(t) < m_u(\theta_-)$ and then it will evolve to the DIS phase, irrespective the subsequent values of θ . Although more pronounced for $k_0 = 20$ than for $k_0 = 12$, but (apparently) less pronounced than the disorder in the control parameter, such case is also featured by a long/remarkable period in which the system exhibits ordering until its vanishing [see e.g. Figs. 4(c) and 5]. As previously, a consecutive sequence of θ_+ 's driving the system to the disordered phase also requires longer times for lower Δt 's and for this reason the time vanishing increases. A discontinuous phase transition between ME and DIS yields at $\theta_+ = \theta_f^-$. Thus, the temporal disorder in inertia also does not suppress the existence of a discontinuous transition and hysteretic branch.

Since the difference between the lowest $A'(f, \theta_-, k_0)$ and the largest $A'(f, \theta_+, k_0)$ is always positive, the phase ORD always prevails over the DIS/ME ones for $k_0 = 12$, $f = 0.12$ and $p = 1/2$, (see e.g. panels (a) – (b) in Fig. 4). The prevalence of the ordered phase over the disordered and metastable phases in such case is a new feature originated from the temporal disorder in the inertia, whose main features are exemplified in the phase diagram Fig. 4(d).

TABLE II. Coefficients $A'(f, \theta, k_0)$ for $f = 0.12$ and $k_0 = 20$ and the resulting phase.

θ	$A'(f, \theta, k_0)$	phase
$3/13 < \theta < 2/7$	0.2295...	ORD
$2/7 \leq \theta < 1/3$	0.0328.	ORD
$1/3 \leq \theta < 3/8$	-0.0683...	ME
$3/8$	-0.0876...	ME
$3/8 < \theta < 7/17$	-0.1176..	DIS

We close this section by mentioning that although not presented for $k_0 = 12$, the competition between ORD and ME/DIS phases can result to a metastable/disordered as exemplified for $k_0 = 20$ (see, e.g. coefficients in Table II).

k_0 (for a given system size N) according to the scheme by Bollobás [32]. Also, the neighborhood of each site has not been altered as the time is changed.

As in the MFT, numerical simulations starts for given initial condition in which a new value of the control parameter (whether f or θ) is sorted from the two possible values (f_-/θ_- and f_+/θ_+) for every interval time ranged between t and $t + \Delta t$. The time evolution of system

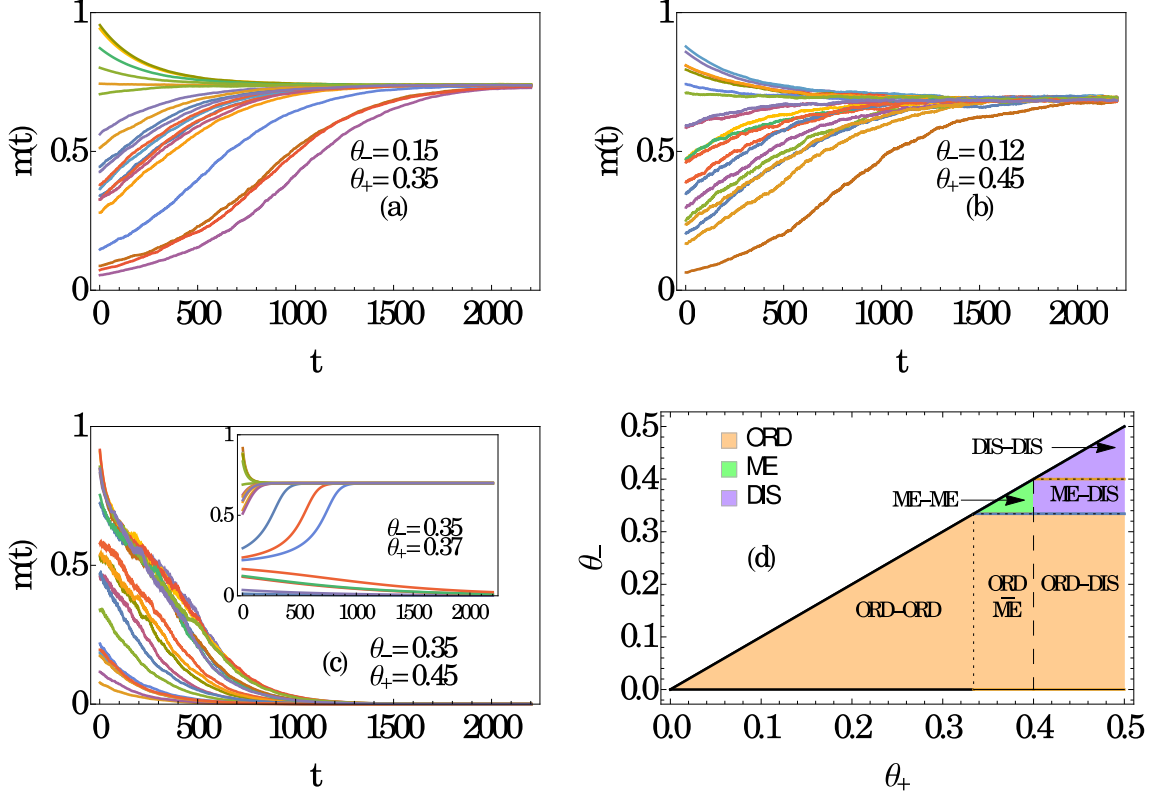


FIG. 4. MFT analysis for the temporal disorder in the inertia: For RR network with values $k_0 = 12$ and $f = 0.12$, panels (a)–(c) exemplify the average time evolution of the m for distinct initial configurations and sorts of inertia $(\theta_-, \theta_+) \in$: (ORD,ME), (ORD,DIS), (ME,DIS), (ME,ME) [inset], respectively. In (d) the phase diagram with dashed and dotted lines representing discontinuous phase transitions lines and crossover between phases, respectively. The resulting phase is represented by distinct colors.

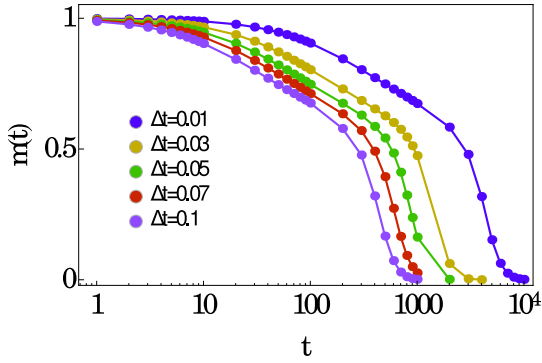


FIG. 5. For $k_0 = 20$, $f = 0.12$, $\theta_- = 0.334 \in$ ME and $\theta_+ = 0.412 \in$ DIS, the average m versus t obtained for $N_D = 10^3$ disorder realizations and distinct Δt 's.

is analyzed until a maximum time t_{\max} that results in a given sequence of $\{f_1, f_2, \dots, f_M\}$ ($\{\theta_1, \theta_2, \dots, \theta_M\}$) in which $t_{\max} = M \times \Delta t$. Such analysis is repeated over $N_D = 10^3 - 10^4$ distinct sequences of temporal disorder. We have considered $\Delta t = 20$ and $t_{\max} = 10^5 - 10^6$.

Resulting phases as well as phase transitions can be identified from two distinct (but equivalent) ways. In the former approach, one considers analysis in the steady state regime in which we start from the ordered phase ($|m|$ close to 1) and f is raised by an amount Δf and the end configuration at f is adopted as the initial condition at $f + \Delta f$. This procedure is repeated until the system reaches the disordered phase at f_f . Conversely, the numerical simulation is restarted for a given value of f constrained in the disordered phase but now f is decreased by Δf until the ordered phase will be reached at f_b . Both forward and backward curves are expected to coincide themselves at both ordered and disordered phases, but not along the metastable branch.

Additionally, the presence of temporal disorder can be more conveniently analyzed (as previously) by inspecting the time evolution of order parameter for distinct initial conditions $0 < |m(0)| \leq 1$. The system will converge for a well defined value in both disordered and ordered phases, respectively, irrespective the initial conditions, whereas it will evolve to two well defined values for f constrained in the metastable branch. Due to the finite size effects, the

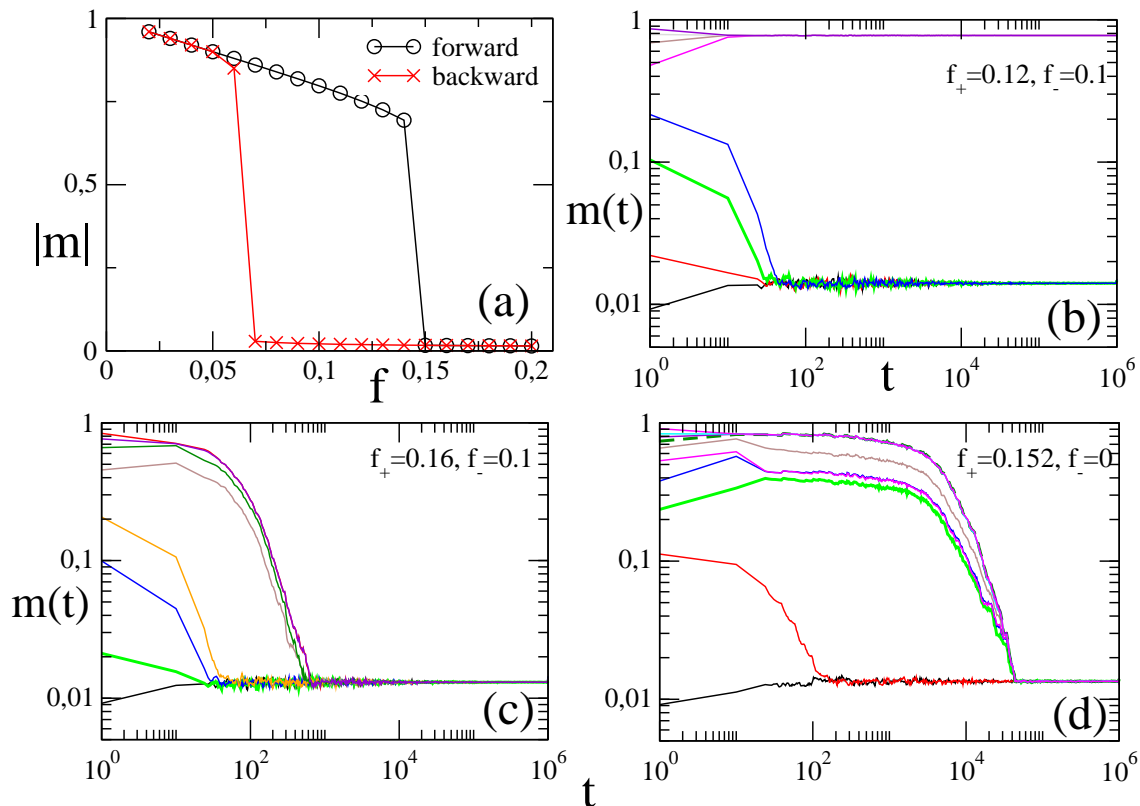


FIG. 6. Panel (a) depicts, for $N = 5000$, $k_0 = 20$ and $\theta = 0.3$, the order parameter $|m|$ versus f for the pure system. Continuous and dotted lines denote the forward and backward increase of f , respectively. Panels (b) – (d) show the average time evolution of the order parameter m (over $N = 10^4$ realizations) for distinct initial conditions $m(0)$ and different sorts of $[f_-, f_+] \in [\text{ME}, \text{ME}], [\text{ME}, \text{DIS}], [\text{ORD}, \text{DIS}]$, respectively.

magnetization never vanishes, but instead, it behaves as $m(t \rightarrow \infty) \sim 1/\sqrt{N}$ in the disordered and metastable phases (for lower $m(0)$).

Although the temporal disorder features are not expected to depend on the values of θ and k_0 , the bistable branch is more pronounced for large connectivities and θ 's and for this reason numerical simulations will be undertaken for $\theta = 0.3$ and $k_0 = 20$, whose hysteretic loop for the pure system was investigated in Ref. [22] and reproduced in Fig. 6(a). As it can be seen, for $f < f_b = 0.060(5)$ the system is constrained in the ordered phase, whereas the bistability yields for $f_b < f < f_f = 0.150(5)$. The disordered phase emerges for $f > f_f$, irrespective

the initial condition. Fig. 6(b) – (d) depicts the main features for temporal disorder in the control parameter for distinct sets of f_+ and f_- belonging to the ORD, ME and DIS phases. In particular, the MFT analysis describes well the findings beyond the MFT, such as the prevalence of the disordered phase over the metastable [Fig.7(a)] for $f_+ < f_f^-$ and the competition between ordered and metastable/disordered phases. More specifically, taking into account that the lowest f_- and f_+ are lower than $2f_b$, the disordered phase always prevails over the ORD one, as illustrated in panel 5(d).

However, due to a finite-size effect the ORD phase always prevails over the metastable for finite N . Since $m(t)$ is finite and proportional to $1/\sqrt{N}$ in the disordered phase, it suffices a long sequence (e.g. a rare fluctuation) of $f = f_-$ for driving the system to the ORD phase. However, such a finite size effect disappears as $N \rightarrow \infty$ and

MFT also describes well the prevalence of the ME phase when $f_+ + f_- > 2f_b$. Since the main features are quite similar to those from MFT, we shall omit the phase diagram. As a final comment, we expect similar trends for other lattice topologies, although the line separating ordered and other phases does not necessarily will obey a derivation like MFT.

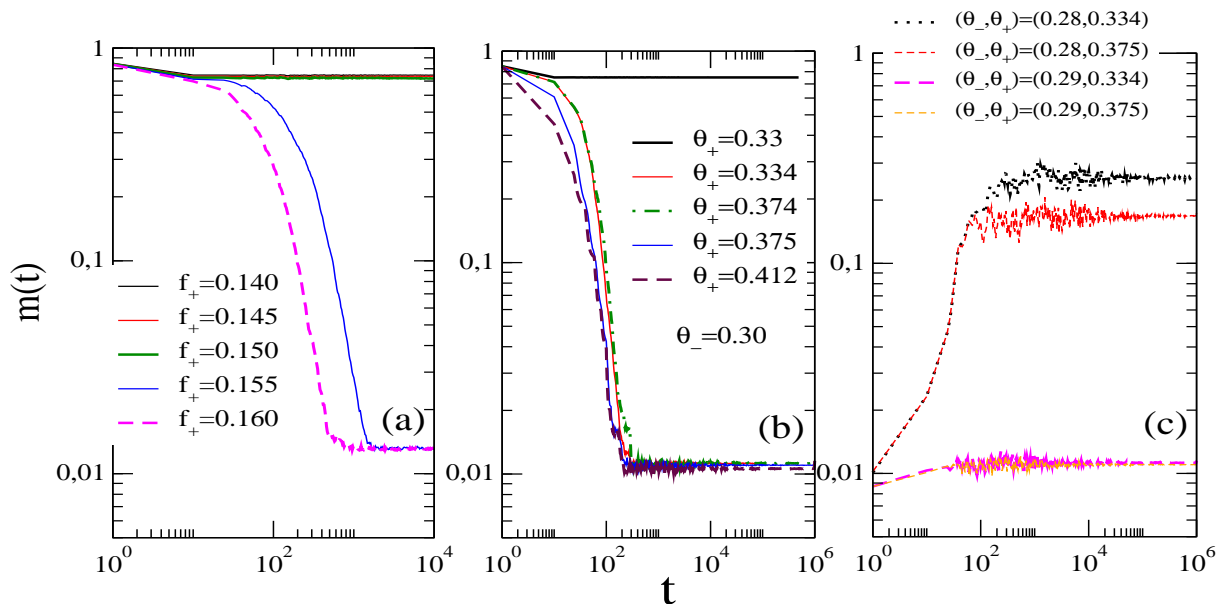


FIG. 7. For a RR network of size $N = 10^4$, $k_0 = 20$ and $\theta = 0.3$, the average time evolution of the order parameter m starting from the ordered state for $f_- = 0.10$ (ME) for distinct f_+ 's. Panel (b) depicts, for $f = 0.12$ and $m(0) = 1$, the time evolution of the average m for $\theta_- = 0.30$ (ME) for distinct θ_+ 's. In (c) the same but for $\theta_- = 0.28$ and 0.29 (both belonging to the ORD phase) and distinct θ_+ 's starting from $m(0) = 10^{-4}$. In all cases, averages are evaluated over $N = 10^3 - 10^4$ realizations

In the last analysis, we exemplify the main features of inertia temporal for $f = 0.12$. Fig. 7(b) shows the competition between metastable and disordered phases

for $f = 0.12$. For the pure version, the hysteretic branch is verified for $2/7 < \theta \leq \theta_f = 1/3$ in which the order-parameter jumps at $\theta > \theta_f$ (see e.g. [31]).

Also in accordance with previous MFT analysis, the competition between ME and DIS phases always suppresses the phase coexistence (see e.g. curves for $\theta_+ > \theta_f$ in Fig. 7(b)) and a discontinuous transition yields at $\theta_+ = \theta_f$. On the other hand, the resulting phase from the competition between ORD and DIS phases will depend on particular values of θ_- and θ_+ . More specifically for $\theta_- = 0.28$ and $1/3 < \theta_+ = 3/8$ the ORD prevails, whereas the system evolves to disordered phase when $\theta_- = 0.29$. Since transition points from MFT and complex topologies are similar for large and k_0 's [22], these above findings can also be understood from coefficients from Table II from which the predominance of ORD and DIS phase holds for $\theta_- = 0.28$ and 0.29 , respectively.

IV. CONCLUSIONS

Based on the MFT, a general description for discontinuous phase transitions in the presence temporal disorder was considered. Our theoretical predictions are general and valid any system displaying a bistable behavior characterized by the existence of a hysteretic branch. The

present study not only confirms previous findings [26] but also extends for other system symmetries and distinct kinds of temporal disorder. Analysis was exemplified in one of the simplest "up-down" system symmetry for two kinds of temporal disorder: inertial majority vote model. Since the inertia plays a fundamental role for the emergence of a discontinuous transition, the effect of its time variation was also investigated. Our main findings can be summarized as follows: Although both kinds of temporal disorder does not suppress existence of a discontinuous phase transition, the phase coexistence is always suppressed when there is a competition between disordered and metastable phases. As for with absorbing phase transitions, the competition between different phases can also lead to an order-parameter vanishing characterized by exponentially large decay times. The mean-field approach describes very well the effect of temporal disorder in complex topologies.

Our findings are general and expected to be valid for other complex structures, such as Erdős Renyi and heterogeneous structures. As a final comment, it will be remarkable to extend such analysis for discontinuous phase transitions in regular structures, which presents an en-

tirely different behavior from complex topologies. In these systems, no hysteretic behavior is presented [24, 25].

V. ACKNOWLEDGMENT

We acknowledge José A. Hoyos for useful suggestions. C. E. F. acknowledges the financial support from FAPESP under grant 2018/02405-1 and J. M. E. acknowledges the financial support from CAPES.

-
- [1] J. Marro and R. Dickman, *Nonequilibrium Phase Transitions in Lattice Models* (Cambridge University Press, Cambridge, 1999).
- [2] M. Henkel, H. Hinrichsen and S. Lubeck, *Nonequilibrium Phase Transitions Volume I: Absorbing Phase Transitions* (Springer-Verlag, The Netherlands, 2008).
- [3] G. Ódor, *Universality In Nonequilibrium Lattice Systems: Theoretical Foundations* (World Scientific, Singapore, 2007).
- [4] T. Vojta and M. Dickison, Phys. Rev. E **72**, 036126 (2005).
- [5] T. Vojta and M. Y. Lee, Phys. Rev. Lett. **96**, 035701 (2006).
- [6] M. M. de Oliveira and S. C. Ferreira, J. Stat. Mech P11001 (2008).
- [7] T. Vojta, A. Farquhar and M. Mast, Phys. Rev. E **79**, 011111 (2009).
- [8] H. Barghathi and T. Vojta, Phys. Rev. Lett **109**, 170603 (2012).
- [9] F. Vazquez, J. A. Bonachela, C. López and M. A. Muñoz, Phys. Rev. Lett. **106**, 235702 (2011).
- [10] R. Martínez-García, F. Vazquez, C. López, and M. A. Muñoz, Phys. Rev. E **85**, 051125 (2012).
- [11] J. A. Hoyos and T. Vojta, Europhysics Lett. **112**, 30002 (2015).
- [12] T. Vojta and R. Dickman, Phys. Rev. E **93**, 032143 (2016).
- [13] H. Barghathi, T. Vojta and J. A. Hoyos, Phys. Rev. E **94**, 022111 (2016).
- [14] C. M. D. Solano, M. M. de Oliveira and C. E. Fiore, Phys. Rev. E **94**, 042123 (2016).
- [15] M.M. de Oliveira and C.E. Fiore Phys. Rev. E **94**, 052138 (2016).
- [16] C. Castellano, S. Fortunato and V. Loretto, Rev. Mod. Phys. **81**, 591 (2009).
- [17] T. Vicsek and A. Zafeiris, Physics Reports **517**, 71 (2012).
- [18] J. A. Acebrón, L. L. Bonilla, C. J. P. Vicente, F. Ritort and R. Spigler, Rev. Mod. Phys. **77**, 137 (2005).
- [19] M. J. de Oliveira, J. Stat. Phys. **66**, 273 (1992).
- [20] H. Chen, C. Shen, G. He, H. Zhang and Z. Hou, Phys. Rev. E **91**, 022816 (2015).
- [21] L. F. Pereira and F. G. B. Moreira, Phys. Rev. E **71**, 016123 (2005).
- [22] H. Chen, C. Shen, H. Zhang, G. Li, Z. Hou and J. Kurths, Rev. E **95**, 042304 (2017).
- [23] P. E. Harunari, M. M. de Oliveira and C. E. Fiore, Phys. Rev. E **96**, 042305 (2017).
- [24] J. M. Encinas, P. E. Harunari, M. M. de Oliveira and C. E. Fiore, Sci. Rep. **8**, 9338 (2018).
- [25] M. M. de Oliveira, M. G. E. da Luz and C. E. Fiore, Phys. Rev. E **97**, 060101(R) (2018).
- [26] C. E. Fiore, M. M. de Oliveira and J. A. Hoyos, Phys. Rev. E **98**, 032129 (2018).
- [27] P. Villa Martín, J. A. Bonachela, and M. A. Muñoz, Phys. Rev. E **89**, 012145 (2014).
- [28] In both logistic equations, the parameter $c > 0$ in order to ensure finite values of the order parameter x .
- [29] C. Castellano and R. Pastor-Satorras, J. Stat. Mech. p. P05001 (2006).
- [30] C. E. F. Noa, P. E. Harunari, M. de Oliveira, and C. E. Fiore, Physical Review E **100**, 012104 (2019).
- [31] J. M. Encinas, H. Chen, M. M. de Oliveira and C. E. Fiore, Phys. A **516**, 563 (2019).
- [32] B. Bollobás, Europ. J. Combin. **1**, 311 (1980).